

# Distributed timing synchronization for sensor networks with coupled discrete-time oscillators

M. Cremaschi, O. Simeone and U. Spagnolini

Dipartimento di Elettronica e Informazione, Politecnico di Milano, I-20133 Milano, Italy

e-mail: simeone, spagnoli@elet.polimi.it

**Abstract**—Physical layer-based distributed timing synchronization among nodes of a wireless network is currently being investigated in the literature as an interesting alternative to packet synchronization. In this paper, we analyze the convergence properties of such a system through algebraic graph theory, by modelling the nodes as discrete-time oscillators and taking into account the specific features of wireless channels (e.g., reciprocity, fading). The analysis is corroborated by numerical results and by comparison with the performance of a practical implementation of the distributed synchronization algorithm over a bandlimited noisy channel.

## I. INTRODUCTION

Distributed timing synchronization among nodes of a wireless network has a wide range of applications, from sensor networks cognitive tasks to over-the-air autonomous inter-base station synchronization [1] or radio-frequency communications among vehicles [2]. In all cases, timing synchronization is needed to appropriately manage the radio resource allocation, e.g., to ensure multiple access. Moreover, in the case of sensor networks, timing synchronization among nodes entails a wealth of novel opportunities that are being currently investigated, such as distributed detection and estimation [3] or cooperative transmission.

Physical layer-based synchronization protocols [4], as opposed to packet-based synchronization [5], are currently being investigated for their unique properties, such as scalability and low computational complexity. The proposal in [4] was inspired by synchrony of periodic activities in autonomous "nodes" observed in biological systems, such as the flashing of fireflies [6]. Accordingly, each node was modelled as a pulse oscillator coupled with all (or some of) the other nodes. This model was extended in [7] by explicitly including the constraint that each node only communicates with its neighbors. In particular, the authors derived a bound on the velocity of convergence by using algebraic graph theory [8].

In this work, we modify the framework for physical layer-based synchronization according to the algorithm employed in [1] and [2]. More specifically, the nodes are modelled as coupled discrete-time oscillators. Each node modifies its current timing synchronization based on a weighted average of the difference in timing synchrony as measured with respect to other nodes. A similar model is commonly employed in the literature on consensus problems for networks of agents [9]. However, here we address the analysis of the network by considering the specific features of the problem at hand related to the nature of the wireless communication channel

among nodes. In particular, here we study the impact of channel reciprocity and randomness (fading) on the wireless links between the nodes. Analysis of the convergence of the synchronization process is carried out by algebraic graph theory as in [7] allowing to relate global convergence properties to the (random) local connectivity of the network.

Moreover, the analysis is corroborated by addressing the issue of a practical implementation of the distributed synchronization algorithm. Simulation results show the theoretical convergence analysis provides an useful tool for validating the performance of a practical synchronization scheme.

## II. PROBLEM FORMULATION

In this Section, we study the system of discrete-time oscillators in the theoretical framework of [1] [9]. Practical implementation issues will be addressed in Sec. V (see also [2]). Let the wireless network be composed of  $K$  nodes, that share a common free oscillation frequency  $1/T$ . In the  $n$ th period of this periodic signal (with respect to any arbitrary reference system), each node, say the  $k$ th, emits a timing pulse at time  $0 \leq T_k(n) < T$ , as shown in fig. 1. This transmitted signal identifies the timing phase of the  $k$ th node. The temporal width of the transmitted pulse (or equivalently the employed bandwidth) has to be selected so as to guarantee the desired resolution of timing synchronization. If pulses emitted by different nodes are not overlapped in time (i.e., if nodes are not synchronous), each node is able to measure the difference between its timing and the corresponding quantities of nearby nodes  $T_i(n) - T_k(n)$ ,  $i \neq k$ .

The signal transmitted by the  $i$ th node and received by the  $k$ th node undergoes flat fading, that is modelled by a random variable  $P_{ki}$  denoting the received power on the  $(i, k)$ th wireless link. Since the network is assumed to be operated with the same carrier frequency, reciprocity of the fading fluctuations implies  $P_{ik} = P_{ki}$ . We will consider the general geometric model

$$P_{ki} = \frac{C}{d_{ki}^\gamma} \cdot G_{ki}, \quad (1)$$

where  $C$  is an appropriate constant,  $d_{ki} = d_{ik}$  is the distance between node  $i$  and node  $k$  and  $G_{ki}$  is a random variable accounting for the fading process.

At the  $(n + 1)$ th period, the  $k$ th node updates its timing

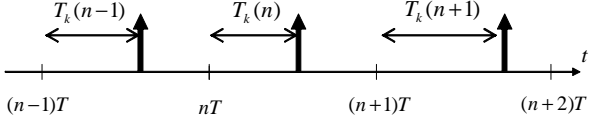


Fig. 1. Timing signal transmitted by the  $k$ th node.

according to the linear equations:

$$T_k(n+1) = T_k(n) + \varepsilon \Delta T_k(n+1) \quad (2a)$$

$$\Delta T_k(n+1) = \sum_{i=1, i \neq k}^K \alpha_{ki} (T_i(n) - T_k(n)). \quad (2b)$$

where  $\varepsilon$  is the step-size ( $0 < \varepsilon < 1$ ) and the linear coefficients  $\alpha_{ki}$  are selected according to [1] as

$$\alpha_{ki} = P_{ki} / \sum_{j=1, j \neq k}^K P_{kj}. \quad (3)$$

This choice accounts for the fact that timings measured over an unreliable channels should not be taken into account when updating the timing phase. Moreover, this design renders the algorithm robust against measurement errors over the fading channels [2] (see also Sec. V). Notice that by using (2b) we are implicitly neglecting the propagation delays among nodes, that are assumed to be smaller than the timing resolution. A method to handle propagation delays is described in [1].

By defining the vector containing the timings of all nodes as  $\mathbf{T}(n) = [T_1(n) \cdots T_K(n)]^T$ , we can express (2) as the discrete-time vector equation

$$\mathbf{T}(n) = \mathbf{A}\mathbf{T}(n-1) \quad (4)$$

where  $\mathbf{A}$  is a  $K \times K$  matrix such that  $A_{ii} = 1 - \varepsilon$  on the main diagonal and  $A_{ij} = \varepsilon \cdot \alpha_{ij}$  for  $i \neq j$ . Notice that *even though we assume channel reciprocity, matrix  $\mathbf{A}$  is not symmetric*. Moreover, by construction, matrix  $\mathbf{A}$  is non-negative and stochastic since the sum of the elements on each row sums to one, or equivalently

$$\mathbf{A} \cdot \mathbf{1} = \mathbf{1}. \quad (5)$$

Model (2) resembles the one considered in the literature on multi-agent coordination (see, e.g., [9]). Synchronization (consensus) is reached when the all the timing  $T_k(n)$  are equal for  $n$  large enough, i.e.,

$$T_1(n) = T_2(n) = \dots = T_k(n) \text{ for } n \rightarrow \infty. \quad (6)$$

On the other hand, the network fractionates into, say, two clusters of synchronization if there exist a permutation function on the nodes' labels,  $\pi(i) : [1, \dots, n] \rightarrow [1, \dots, n]$  such that for  $n$  large enough

$$\begin{aligned} T_{\pi(1)}(n) &= \dots = T_{\pi(r)}(n) \\ T_{\pi(r+1)}(n) &= \dots = T_{\pi(K)}(n). \end{aligned} \quad (7)$$

The number of nodes in the two clusters is  $r$  and  $K - r$  respectively. The definition above generalizes naturally to more than two clusters.

In the following Sections, we will related the properties of convergence of the dynamic system (2) to the algebraic properties of the system matrix  $\mathbf{A}$  and of the associated graph (to be introduced in the following Section). As a preliminary remark, we notice that the convergence properties of the dynamic system depend on the largest absolute value of the eigenvalues of  $\mathbf{A}$ . Since, according to the Gershgorin theorem [11], all the eigenvalues  $\lambda_i$  ( $i = 1, \dots, K$ ) of  $\mathbf{A}$  satisfy the condition  $|\lambda_i - (1 - \varepsilon)| \leq \varepsilon$ , the dominant eigenvalue is  $\lambda_1 = 1$  (recall (5)). Moreover, the remaining eigenvalues can be at most equal to 1. Multiplicity of the eigenvalue  $\lambda_1 = 1$  will play a key role in the analysis of convergence, as shown below.

### III. CONVERGENCE ANALYSIS

The goal of this Section is to determine the conditions under which the network converges to a unique cluster or to multiple clusters of synchronization for a fixed realization of the fading variable, i.e., matrix  $\mathbf{A}$  is assumed to be deterministic. This amounts to setting  $G_{ki} = 1$  in (1). We will define the conditions of convergence in terms of the properties of the graph associated to the wireless network under study, or equivalently in terms of the system matrix  $\mathbf{A}$ .

The wireless network can be represented by the weighted directed graph  $\mathcal{G} = (\mathcal{V}, \mathcal{E}, \mathcal{A})$  of order  $K$ , where  $\mathcal{V} = \{1, \dots, K\}$  is the set of nodes and  $\mathcal{E} \subseteq \mathcal{V} \times \mathcal{V}$  is the set of edges weighted by the off-diagonal elements of the adjacency matrix  $\mathcal{A} = [\alpha_{ij}]$ . The edge connecting the  $i$ th and the  $j$ th nodes,  $i \neq j$ , belongs to  $\mathcal{E}$  if and only if  $\alpha_{ij} > 0$ . Notice that *the graph is directed* ( $\alpha_{ij} \neq \alpha_{ji}$  for  $i \neq j$ ), *even though fading links are reciprocal* ( $P_{ij} = P_{ji}$  for  $i \neq j$ ). Moreover, notice that the system matrix reads  $\mathbf{A} = \mathbf{I} - \varepsilon \mathcal{A}$ . The main result of this Section (Theorem 1) relates the convergence properties of distributed synchronization with the connectivity of the associated graph  $\mathcal{G}$  (or equivalently to the reducibility of matrix  $\mathbf{A}$ ).

*Definition 1:* A graph  $\mathcal{G}$  is said to be strongly connected if there exists a path (i.e., a collection of edges in  $\mathcal{E}$ ) that links every pair of nodes.

It can be proved that strong connectivity of graph  $\mathcal{G}$  is equivalent to the irreducibility of matrix  $\mathbf{A}$  [11].

*Definition 2:* A  $K \times K$  matrix  $\mathbf{A}$  is said to be *reducible* if there exists a  $K \times K$  permutation matrix  $\mathbf{P}$  and an integer  $r > 0$  such that

$$\mathbf{P}^T \mathbf{A} \mathbf{P} = \begin{bmatrix} \mathbf{B} & \mathbf{C} \\ \mathbf{0} & \mathbf{D} \end{bmatrix}, \quad (8)$$

where  $\mathbf{B}$  is  $r \times r$ ,  $\mathbf{D}$  is  $K - r \times K - r$ ,  $\mathbf{C}$  is  $r \times K - r$  and the zero matrix  $\mathbf{0}$  is  $K - r \times r$ . A matrix  $\mathbf{A}$  is called irreducible if it is not reducible.

The degree of irreducibility of a matrix  $\mathbf{A}$ , or equivalently of strong connectivity of the associated graph  $\mathcal{G}$ , can be measured by the following quantity (see, e.g., [10])

$$\sigma = \min_{\mathcal{V}_1, \mathcal{V}_2} \left( \sum_{i \in \mathcal{V}_1, j \notin \mathcal{V}_1} \alpha_{ij} + \sum_{i \in \mathcal{V}_2, j \notin \mathcal{V}_2} \alpha_{ij} \right) \quad (9)$$

where the minimum is taken over all non-empty proper subsets

of  $\mathcal{V}$ ,  $\mathcal{V}_1 \cap \mathcal{V}_2 = \emptyset$  ( $\mathcal{V}_1 \cup \mathcal{V}_2 = \mathcal{V}$ ). It can be shown that  $\sigma = 0$  if and only if the matrix  $\mathbf{A}$  is reducible, or the associated graph  $\mathcal{G}$  is not strongly connected.

The main result of this Section can be now stated as follows.

*Theorem 1:* (i) The distributed synchronization (2) converges to a unique cluster of synchronized nodes,  $T_1(n) = \dots = T_k(n) = T_\infty$  for  $n \rightarrow \infty$ , if and only if the associated weighted directed graph  $\mathcal{G}$  is strongly connected, or equivalently if system matrix  $\mathbf{A}$  is irreducible. (ii) In this case, the system (4) converges to

$$T_\infty = \mathbf{v}^T \mathbf{T}(0), \quad (10)$$

where  $\mathbf{v}$  is the normalized left eigenvector of matrix  $\mathbf{A}$  corresponding to eigenvalue 1:  $\mathbf{A}^T \mathbf{v} = \mathbf{v}$  with  $\mathbf{1}^T \mathbf{v} = 1$ .

An immediate consequence of the Theorem 1 is that the timing vectors converge to the average of their initial values  $\mathbf{T}(0)$  if and only if the system matrix  $\mathbf{A}$  is doubly stochastic (i.e., if  $\mathbf{A}^T$  is stochastic as well). In fact, in this case  $\mathbf{A}^T \mathbf{1} = \mathbf{1}$  and vector  $\mathbf{v}$  in (10) reads  $\mathbf{v} = 1/K \cdot \mathbf{1}$ . In sensor networks, this result is of interest in applications where the steady state value of synchronization is used in order to infer the status of the process monitored by the sensor (e.g., change detection [3]).

*Proof:* The proof of part (i) of Theorem 1 is available in the literature for applications where the graph  $\mathcal{G}$  associated to the dynamic system (4) is undirected [8]. In the case of a directed graph, strong connectivity can generally be proved to be only a sufficient condition for synchronization. However, in the wireless fading case with reciprocal channels the result can be proved as shown in the following. The second part (ii) of Theorem 1 follows from a result derived, among the others, in [9].

As explained above, in order to prove Theorem 1, we only need to show that strong connectivity is also a necessary condition for synchronization. As a by-product, the proposed proof brings insight into the formation of multiple clusters of synchronization (7). Let us assume that  $\mathbf{A}$  is reducible (or equivalently the associated graph  $\mathcal{G}$  is not strongly connected). Then, by definition, there exists a permutation matrix  $\mathbf{P}$  and an integer  $r > 0$  such that (8) holds. But if  $\alpha_{ij} = 0$  in  $\mathbf{A}$  then for reciprocity  $P_{ij} = P_{ji} = 0$  and then  $\alpha_{ji} = 0$  ( $i \neq j$ ). Therefore, the  $r \times K - r$  matrix  $\mathbf{C}$  in (8) has all zero entries. Since the permuted matrix  $\mathbf{P}^T \mathbf{A} \mathbf{P}$  is non-negative and stochastic, so are submatrices  $\mathbf{B}$  and  $\mathbf{D}$ . By applying the permutation function  $\pi(k) = \mathbf{P}_k [1 \dots K]^T$ , where  $\mathbf{P}_k$  is the  $k$ th row of matrix  $\mathbf{P}$ , to the nodes' labels, we can write the system (4) as

$$\tilde{\mathbf{T}}(n) = \begin{bmatrix} \mathbf{B} & \mathbf{0} \\ \mathbf{0} & \mathbf{D} \end{bmatrix} \tilde{\mathbf{T}}(n-1), \quad (11)$$

where  $\tilde{\mathbf{T}}(n) = \mathbf{P} \mathbf{T}(n)$ . Therefore, the set of  $r$  nodes  $\{\pi(1), \dots, \pi(r)\}$  evolves independently from the remaining nodes  $\{\pi(r+1), \dots, \pi(K)\}$ . Now, if either  $\mathbf{B}$  or  $\mathbf{D}$  are reducible, the reasoning above can be iterated bringing to the formation of multiple independent set of nodes evolving separately. At the end of this procedure, the system matrix can be written as a block matrix with irreducible stochastic

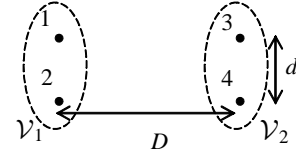


Fig. 2. The rectangular topology considered in the example in Sec. III-A.

blocks on the diagonal. Without loss of generality, let us then assume that  $\mathbf{B}$  and  $\mathbf{D}$  are irreducible. From the first part of the proof (see also Appendix-A), it follows the two cluster of  $r$  and  $(K-r)$  nodes synchronize among themselves according to (7). Moreover, the steady state values of the timing vectors depend on the left eigenvectors of  $\mathbf{B}$  and  $\mathbf{D}$  according to (10):

$$\begin{aligned} \lim_{n \rightarrow \infty} T_{\pi(i)}(n) &= \mathbf{v}_B^T \tilde{\mathbf{T}}_r(0), \quad i = 1, \dots, r & (12a) \\ \lim_{n \rightarrow \infty} T_{\pi(i)}(n) &= \mathbf{v}_D^T \tilde{\mathbf{T}}_{K-r}(0), \quad i = r+1, \dots, K & (12b) \end{aligned}$$

where  $\mathbf{B}^T \mathbf{v}_B = \mathbf{v}_B$ ,  $\mathbf{D}^T \mathbf{v}_D = \mathbf{v}_D$ ,  $\tilde{\mathbf{T}}_r(n) = [T_{\pi(1)}(n) \dots T_{\pi(r)}(n)]$  is the  $r \times 1$  vector collecting the first  $r$  entries of  $\tilde{\mathbf{T}}(n)$  and  $\tilde{\mathbf{T}}_{K-r}(n) = [T_{\pi(r+1)}(n) \dots T_{\pi(K)}(n)]$  is the  $K-r \times 1$  vector collecting the remaining entries. ■

As stated in the introduction, the convergence of the dynamic system at hand could be also studied in terms of the subdominant eigenvalue of matrix  $\mathbf{A}$ , similarly to approach commonly adopted in the context of the analysis of Markov chains. In particular, the following results can be proved relating convergence to the multiplicity of eigenvalue 1.

*Theorem 2:* The distributed synchronization (2) converges to a unique cluster of synchronized nodes as in (6) if and only if the subdominant eigenvalue  $\lambda_2 \neq 1$ .

*Proof:* By recalling Theorem 1, it is enough to prove that: i) if  $\lambda_2 = 1$  then the graph is not strongly connected; ii) if the graph is not strongly connected then  $\lambda_2 = 1$ . Part i) can be proved similarly to [9]; however, in Appendix-B we give an alternative proof based on the measure  $\sigma$  in (9) of irreducibility of  $\mathbf{A}$ . Part ii) does not hold in general for problems with directed graphs but it is easily shown under the reciprocity assumption similarly to Theorem 1. ■

#### A. Numerical results

Here we present a numerical example to corroborate the analysis discussed above. A network of  $K = 4$  nodes is considered where the nodes are divided into two groups,  $\mathcal{V}_1 = \{1, 2\}$  and  $\mathcal{V}_2 = \{3, 4\}$ , as in fig. 2. The initial values  $T_k(0)$  are set to  $\mathbf{T}(0)/T = [0.1 \ 0.4 \ 0.6 \ 0.8]^T$ . The path loss exponent is  $\gamma = 3$ , whereas the value of  $C$  in (1) does not affect the performance and is therefore irrelevant according to definition (3). Fig. 3 shows the timing vector  $\mathbf{T}(n)$  versus  $n$  for  $D/d = 2$  and  $\varepsilon = 0.3$ . Notice that we are considering the normalized distance  $D/d$  since the algorithm (2) is only sensitive to relative distances. After a transient where the nodes tend to synchronize in pairs within the two groups, the system reaches the steady state to the average value  $T_\infty/T = 0.475$ ,

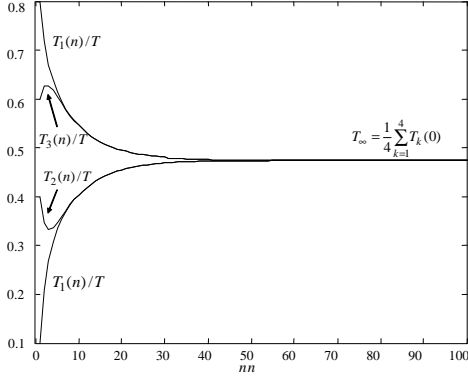


Fig. 3. The timing  $T_k(n)$  versus time  $n$  for the rectangular topology in fig. 2 with  $D/d = 2$  ( $\varepsilon = 0.3$ ,  $\gamma = 3$ ,  $K = 4$ ).

as stated in Theorem 1, since the system matrix is easily shown to be doubly stochastic for this specific example.

In order to quantify the rate of convergence, from Theorem 2, we notice that the convergence of the synchronization protocol (2) depends on the subdominant eigenvalue  $\lambda_2$ . In particular, as it is well known from the theory of dynamic system, the rate of convergence is ruled by a term proportional to  $|\lambda_2|^n$ . If we define a threshold  $T_o$ , we could say that the protocol reaches the steady state condition at the time instant  $n_o$  for which  $|\lambda_2|^{n_o} = T_o$ :  $n_o = \log T_o / \log |\lambda_2|$ . Therefore, we can take

$$v = -\log |\lambda_2| \quad (13)$$

as a measure of the rate of convergence of the algorithm. Fig. 4 shows the rate of convergence  $v$  versus the normalized distance  $D/d$  for  $\varepsilon = 0.3, 0.7$ . As expected the rate  $v$  decreases with increasing  $D/d$  and decreasing  $\varepsilon$ . Along with  $v$ , fig. 4 shows the measure of irreducibility (or strong connectivity)  $\sigma$  (9) as dashed lines. It is interesting to note that the rate of convergence  $v$  and the measure of irreducibility  $\sigma$  have the same behavior as a function of  $D/d$  and  $\varepsilon$ . This confirms that convergence is strictly related to the connectivity properties of the associated graph, as proved in Theorem 1.

#### IV. EFFECT OF FADING

In this Section, the effect of fading on the rate of convergence  $v$  is studied via simulation for linear, ring and star topologies (see fig. 5, recall that convergence depends only on relative distances). Rayleigh fading is assumed, i.e., the fading amplitude  $g_{ki}$  in (1) is assumed to be an exponentially distributed random variable with unit average. Fig. 6 plots the average rate of convergence  $E[v]$  (where the average  $E[\cdot]$  is taken with respect to the distribution of fading) for the three networks versus the number of nodes  $K$  ( $\varepsilon = 0.3$ ). Notice that for  $K = 2$  the three networks coincide and recall that only relative distances are of concern for the behavior of the system (2). As it is expected the star topology has the largest rate of convergences whereas the linear network yields the slowest convergence.

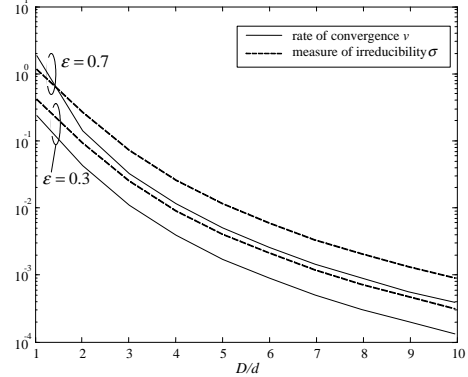


Fig. 4. The rate of convergence  $v$  (13) and the measure of irreducibility  $\sigma$  (9) versus  $D/d$  for the rectangular topology in fig. 2 ( $\varepsilon = 0.3, 0.7$ ,  $\gamma = 3$ ,  $K = 4$ ).

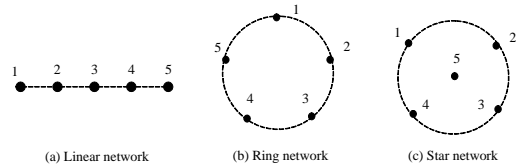


Fig. 5. The linear, ring and star networks ( $K = 5$ ).

#### V. PRACTICAL IMPLEMENTATION OF DISTRIBUTED COUPLED DISCRETE-TIME OSCILLATORS

In this Section, we present a practical scheme that implements the distributed synchronization over a bandlimited noisy channel. The scheme follows [2], to which we refer to a more thorough presentation. A carrier frequency is dedicated to the synchronization channel, where each node, say the  $k$ th, transmits square root raised cosine pulses (centered) at (absolute) times  $\bar{T}_k(n)$ . The transmitted waveform occupies a bandwidth  $B = (1 + \delta)/T_s$  where  $T_s$  is the symbol period and  $\delta$  the roll-off factor. The symbol period  $T_s$  defines the timing resolution of the system. Each node works in the half-duplex mode and measures the received signal on an interval of duration  $T$  around the current timing instant  $\bar{T}_k(n)$ , i.e., within  $t \in (\bar{T}_k(n) - T/2, \bar{T}_k(n) + T/2)$ . The receiver performs baseband filtering matched to the transmitted waveform and then samples the received signal at symbol frequency  $1/T_s$ . Based on the  $N = T/T_s$  samples received, the node computes the update  $\bar{T}_k(n+1) = \bar{T}_k(n) + T + \Delta\bar{T}_k(n)$  similarly to (2a)-(2b), as explained below.

The discrete-time baseband signal received by the  $k$ th node in the  $n$ th time period reads  $(-N/2 < m \leq N/2)$

$$y_k(n, m) = \sum_{i=1, i \neq k}^K \sqrt{E_{ki}} \cdot \beta_{ki} \cdot g(mT_s - \bar{T}_{i,k}(n)) + w(n, m) \quad (14)$$

where the average energy per symbol reads  $E_{ki} = C/d_{ki}^2 \cdot T_s$  (recall (1));  $\beta_{ki}$  denotes the Rayleigh fading coefficient, that

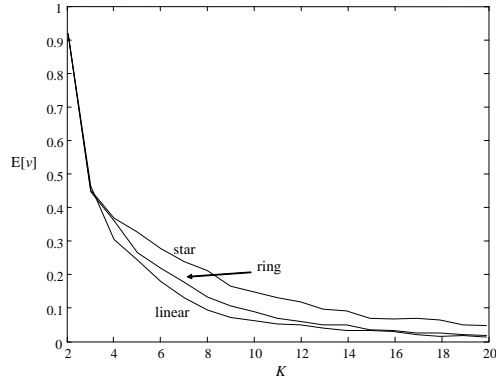


Fig. 6. Average rate of convergence  $E[v]$  for the linear, ring and star network in fig. 5 versus the number of nodes  $K$  ( $\varepsilon = 0.3$ ,  $\gamma = 3$ ).

is a zero-mean and unit-power complex (circularly symmetric) Gaussian random variable with  $|\beta_{ki}|^2 = G_{ki}$ ; and  $w(n, m)$  is the additive (circularly symmetric) Gaussian noise with zero mean and power  $N_0$ . Moreover,  $\tilde{T}_{i,k}(n) = \bar{T}_i(n) - \bar{T}_k(n)$  is the timing difference between the node  $i$  and the receiving node  $k$ . Notice that the sample in  $m = 0$ , and possibly nearby samples, are not measured due to the half-duplex constraint ( $m = 0$  corresponds to the timing instant  $\bar{T}_k(n)$ ) and the switching time between receive and transmit mode of node  $k$ . A simple implementation of protocol (2a)-(2b) then leads to:

$$\Delta \bar{T}_k(n) = \sum_{m \in \mathcal{J}} \bar{\alpha}_{km} \cdot m, \quad (15a)$$

$$\bar{\alpha}_{km} = \frac{|y_k(n, m)|^2}{\sum_{i \in \mathcal{J}} |y_k(n, i)|^2} \quad (15b)$$

where  $\mathcal{J}$  is the subset of time instants  $m \in (-N/2, N/2]$  for which the received signal  $|y_k(n, m)|^2$  is above a threshold selected so as to ensure a given probability of false alarm as in [2].

For the example of Sec. III-A (no fading) and the algorithm explained above, fig. 7 shows the standard deviation of timing vectors as compared to the steady state value  $T_\infty$ :  $v(n) = \sqrt{1/4 \cdot \sum_{k=1}^4 (T_k(n) - T_\infty)^2}$ , versus  $n$  ( $\varepsilon = 0.5$ ). All nodes transmit the same power and the signal to noise ratio for transmission to the closest node (e.g., from 2 to 1) is set to  $SNR = E_{12}/N_0 = 15dB$ , the probability of false alarm to  $10^{-3}$  and  $D/d = 2$ . The performance of the synchronization algorithm is compared with the theoretical performance of the system (2). The gap between the two curves is due to the finite signal to noise ratio and the finite resolution of the system.

## VI. CONCLUSION

In this work, the convergence properties of physical layer-based distributed timing synchronization based on discrete-time coupled oscillators has been investigated using tools from algebraic graph theory. The analysis has been corroborated by numerical results and by comparison with the performance of

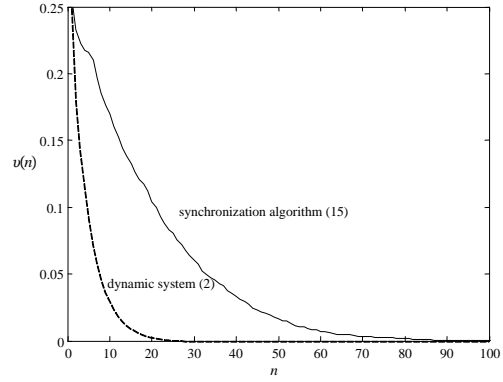


Fig. 7. Standard deviation  $v(n)$  of the timing signals with respect to the steady state value  $T_\infty$  for the synchronization algorithm over a bandlimited Gaussian channel (15) and for the dynamic system (2) (network in fig. 2,  $SNR = 15dB$ ,  $D/d = 2$ ,  $\varepsilon = 0.5$ ,  $\gamma = 3$ ,  $K = 4$ ).

a practical implementation of the distributed synchronization algorithm over a bandlimited noisy channel.

## VII. APPENDIX: PROOF OF THEOREM 2

We need to prove that if  $\lambda_2 = 1$  then the graph is not strongly connected. Toward this goal, we note that we have the following bound on the measure of irreducibility  $\sigma$  (9) [10]:

$$|1 - \lambda_2| \geq \sigma \frac{8}{2K^2 + (-1)^K - 1}, \quad (16)$$

from which it easily follows that if  $\lambda_2 = 1$ ,  $\sigma = 0$  and thus the graph is not strongly connected.

## REFERENCES

- [1] F. Tong and Y. Akaiwa, "Theoretical analysis of interbase-station synchronization systems," *IEEE Trans. Commun.*, vol. 46, no. 5, pp. 590-594, 1998.
- [2] E. Sourour and M. Nakagawa, "Mutual decentralized synchronization for intervehicle communications," *IEEE Trans. Veh. Technol.*, vol. 48, no. 6, pp. 2015-2027, Nov. 1999.
- [3] V. V. Veeravalli, "Decentralized quickest change detection," *IEEE Trans. Inform. Theory*, vol. 47, no. 4, pp. 1657-1665, May 2001.
- [4] Y.-W. Hong, A. Scaglione, "A scalable synchronization protocol for large scale sensor networks and its applications," *IEEE Journal Selected Areas Commun.*, vol. 23, no. 5, pp. 1085-1099, May 2005.
- [5] F. Sivrikaya and B. F. Yener, "Synchronization of pulse-coupled biological oscillators," *IEEE Network*, vol. 18, no. 4, pp. 45-50, July-Aug. 2004.
- [6] R. E. Mirollo and S. H. Strogatz, "SIAM Journal on Applied Mathematics", vol. 50, no. 6, pp. 1645-1662, Dec. 1990.
- [7] D. Lucarelli and I.-J. Wang, "Decentralized synchronization protocols with nearest neighbor communication," in *Proc. ACM SenSys 2004*, Baltimore, Nov. 2004.
- [8] C. Godsil and G. Royle, *Algebraic Graph Theory*, Springer-Verlag, 2001.
- [9] R. Olfati-Saber and R. Murray, "Consensus problems in networks of agents with switching topology and time-delays," *IEEE Trans. Automatic Control*, vol. 49, no. 9, pp. 1520-1533, Sept. 2004.
- [10] X. Zhang and R. Lou, "Upper bound for the non-maximal eigenvalues of irreducible nonnegative matrices," *Czechoslovak Mathematical Journal*, no. 52, pp. 537-544, 2002.
- [11] R.A. Horn and C.R. Johnson, *Matrix Analysis*, Cambridge University Press, 1985.